

Julia A. Bahteeva · Ilia A. Leonidov
Mikhail V. Patrakeev · Edward B. Mitberg
Victor L. Kozhevnikov · Kenneth R. Poeppelmeier

High-temperature ion transport in $\text{La}_{1-x}\text{Sr}_x\text{FeO}_{3-\delta}$

Received: 11 April 2003 / Accepted: 29 September 2003 / Published online: 12 February 2004
© Springer-Verlag 2004

Abstract The conductivity of the entire solid solution $\text{La}_{1-x}\text{Sr}_x\text{FeO}_{3-\delta}$, where $x=0.2, 0.4, 0.5, 0.7$ and 0.9 , in the oxygen partial pressure range 10^{-19} to 0.5 atm and temperatures between 750 and 950 °C is reported. The analysis of the isothermal pressure dependences of the conductivity reveal that the lanthanum-strontium ferrites can be characterized as mixed ion-electron conductors in the low-oxygen pressure/high-oxygen deficiency limit. The partial contribution to conductivity from oxygen ions increases with strontium content and attains a maximal value at $x=0.5$. Further increase in doping results in the development of oxygen vacancy ordering phenomena and deterioration of the conducting properties.

Keywords Electron conductivity · Lanthanum-strontium ferrite · Oxygen conductivity · Oxygen-vacancy ordering

Introduction

The lanthanum-strontium ferrite solid solution $\text{La}_{1-x}\text{Sr}_x\text{FeO}_{3-\delta}$ has been intensively studied. This interest is related to the potential of these oxides for such applications as catalysts, high-temperature fuel cell electrodes and membrane materials. Features of the crystalline structure and peculiarities of the defect state

of these materials have been extensively reported [1, 2, 3, 4, 5, 6, 7, 8, 9, 10, 11, 12]. At the same time, a number of controversies exist concerning the transport properties. For example, Mizusaki et al. [1, 2] analyzed their data for conductivity in oxides with $x=0, 0.1$ and 0.25 assuming only an electronic component. Later, Teraoka et al. [3] reported a high semi-permeability of oxygen, thus showing considerable oxygen-ion contribution to the conductivity in ferrites with a large strontium content. In contrast, Kim et al. [10] supposed a negligibly small ion contribution in their analysis of conductivity in specimens with $x=0.6$ and 0.8 . The studies by ten Elshof et al. [11, 12] also demonstrated appreciable oxygen semi-permeability, i.e. oxygen ion contribution to the conductivity, in oxides with $x=0.1-0.4$. Overall, considerable disagreement exists on the magnitude of the ion component in the conductivity. Moreover, most papers on transport properties involve relatively narrow concentration limits where either minimal strontium or strontium-rich compositions were studied. In addition, given the different temperatures and oxygen pressure intervals utilized, it is difficult to make a comparison of the results which have been reported and to delineate the influence of the acceptor doping upon transport properties over the entire range of the solid solution. Also, the ion conductivity was measured mainly in the high-pressure extreme, while data at low partial pressures of oxygen remain scarce. The present work was directed, therefore, at studying the influence of acceptor doping on the high-temperature conductivity in $\text{La}_{1-x}\text{Sr}_x\text{FeO}_{3-\delta}$, where $x=0.2, 0.4, 0.5, 0.7$ and 0.9 , over a wide range of oxygen partial pressures. Particular attention is given to the data analysis below 10^{-6} atm.

Experimental

The samples used in this study were prepared by solid-state reactions. Starting materials were the oxides Fe_2O_3 (99.2%) and La_2O_3 (99.96%) and strontium carbonate, SrCO_3 (99.94%). The raw materials were pre-calcined to remove adsorbates, weighed in

Presented at the OSSEP Workshop "Ionic and Mixed Conductors: Methods and Processes", Aveiro, Portugal, 10–12 April 2003

J. A. Bahteeva · I. A. Leonidov · M. V. Patrakeev
E. B. Mitberg · V. L. Kozhevnikov (✉)
Institute of Solid State Chemistry, Ural Branch of RAS,
Pervomaiskaia 91, 620219 Ekaterinburg, Russia
E-mail: kozhevnikov@imp.uran.ru
Tel.: +7-3432-783661
Fax: +7-3432-740003

K. R. Poeppelmeier
Department of Chemistry, Northwestern University,
2145 Sheridan Road, Evanston, IL 60208, USA

desirable amounts and thoroughly mixed with a mortar and pestle with addition of ethanol. The mixtures were pressed into pellets and fired at 750–1300 °C in air. The materials were crushed into powder, pressed and fired several times with a gradual increase in temperature before single-phase specimens were obtained. Phase purity and determination of the lattice parameters were carried out with X-ray powder diffraction ($\lambda = 1.54178 \text{ \AA}$). The reduction experiments and studies of oxygen-content changes in the specimens as a function of temperature were carried out with a Setaram TG-DTA-92 thermoanalyzer in an atmosphere containing 5% H_2 and 95% He. The residual water vapor in the gas mixture was frozen with liquid nitrogen before passing the gas into the thermoanalyzer. The reduction process was carried out until the sample weight was constant, indicating complete reduction of the ferrite into iron metal, SrO and La_2O_3 . The respective weight loss was used to calculate the oxygen content in the starting ferrite. Also, a vertical tubular furnace was used for high-temperature treatment of specimens in different atmospheres. When necessary, quenching was performed by dropping samples into a crucible with liquid gallium that rested in the lower end of the tubular compartment at room temperature.

A part of the synthesized materials was ball-milled in ethanol media and pressed into discs under 2 kbar uniaxial load. The disks were sintered in air at 1300–1350 °C for 10 h to a density no less than 90% of theoretical. Rectangular bars $2 \times 2 \times 15 \text{ mm}$ were cut from the sintered discs for the four-probe d.c. conductivity measurements. Potential probes and current leads were made of 0.3 mm Pt wire and tightly wound to the specimen with 7 and 12 mm spacing, respectively. The wired specimen was sealed under an atmosphere containing 50% O_2 and 50% CO_2 in the measuring cell of cubically stabilized zirconia. The cell was equipped with two pairs of Pt electrodes. One pair was used as an oxygen pump in order to change and maintain oxygen partial pressure ($p\text{O}_2$), while the other was utilized as an oxygen sensor in order to independently control the $p\text{O}_2$ inside the cell. The assembly was set in the isothermal zone of a tubular furnace where the temperature of the experiment was maintained. More experimental details are given elsewhere [13]. The electrical parameters were measured with a high-precision voltmeter Solartron 7081. Computer-controlled operation of the oxygen pump and sensor provided precise variation and maintenance of the partial oxygen pressure in the cell. The measurements were carried out in the mode of decreasing oxygen partial pressure in isothermal runs. The relaxation time after a change in the oxygen pressure over a sample varied and was dependent on the temperature and oxygen partial pressure range. The criterion for achieving equilibrium was accepted as a relaxation rate of less than 0.1% per minute in the logarithm of the conductivity under a fixed oxygen pressure inside the cell.

Results and discussion

Crystal structure and oxygen content

The X-ray powder diffraction patterns of the as-synthesized samples of $\text{La}_{1-x}\text{Sr}_x\text{FeO}_{3-\delta}$ show formation of perovskite-like structures at all strontium contents. In agreement with previous reports [6, 14], the crystal lattices correspond to orthorhombic, rhombohedral and cubic symmetry for specimens with $x = 0.2$; 0.4, 0.5 and 0.7; and 0.9, respectively. The unit cell parameters are shown in Table 1. The oxygen content changes on heating in a 5% $\text{H}_2/95\%$ He atmosphere are shown in Fig. 1. Most of the reduction occurs by 500 °C. At the same time, the weight changes are small in the temperature range 500–750 °C, where the oxygen content remains close to $(3-\delta \approx 3-x/2)$. The X-ray powder

Table 1 Unit cell data at room temperature for specimens $\text{La}_{1-x}\text{Sr}_x\text{FeO}_{3-\delta}$ equilibrated at 950 °C and quenched in air

x	Symmetry	a (Å)	b (Å)	c (Å)
0.2	Orthorhombic	5.523(1)	5.550(1)	7.817(2)
0.4	Rhombohedral ^a	5.519(1)	–	13.420(3)
0.5	Rhombohedral	5.503(1)	–	13.417(3)
0.7	Cubic	3.873(1)	–	–
0.9	Cubic	3.866(1)	–	–

^aHexagonal setting

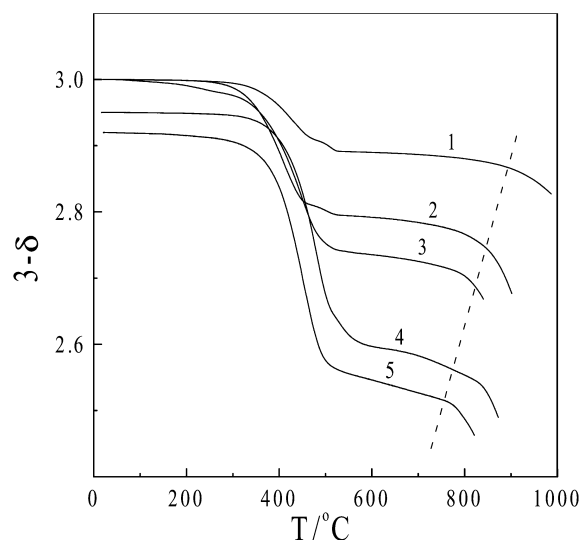


Fig. 1 The weight changes for $\text{La}_{1-x}\text{Sr}_x\text{FeO}_{3-\delta}$ on heating in an atmosphere containing 5% H_2 and 95% He; $x = 0.2$ (1), 0.4 (2), 0.5 (3), 0.7 (4) and 0.9 (5). The dashed line shows approximately the decomposition temperature

diffraction patterns of the samples, after cooling from 700 °C in the TG apparatus, are given in Fig. 2. Heating to still higher temperatures initiates further loss of oxygen and partial reduction of iron to the +2 oxidation state, which results in formation of oxygen-deficient oxides, $\text{La}_{1-x}\text{Sr}_x\text{FeO}_{3-x/2-\delta}$, and then to the loss of stability and structural collapse.

The sample with $x = 0.2$ retains an orthorhombic perovskite-like structure after firing at 700 °C in the strongly reducing hydrogen/helium mixture, as can be seen from Fig. 2. The X-ray reflections can be indexed with a rhombohedral unit cell for $x = 0.4$ and 0.5. The oxygen vacancies appear to be randomized in the composition range $x \leq 0.5$. Quite differently, the compound with $x = 0.7$ acquires an orthorhombic triple perovskite structure where oxygen vacancies order to form layers of iron-oxygen tetrahedra (T) alternating along the b -axis with the layers of iron-oxygen octahedra (O) as $\cdots\text{OO}\text{-TOOT}\cdots$ [15]. The diffraction pattern for $\text{La}_{0.1}\text{Sr}_{0.9}\text{FeO}_{2.55}$ is close to that of the brownmillerite-like ferrite $\text{Sr}_2\text{Fe}_2\text{O}_5$, where vacancy ordering results in the stacking sequence $\cdots\text{OTOT}\cdots$ along the b -axis [16, 17]. The respective unit cell parameters are given in Table 2.

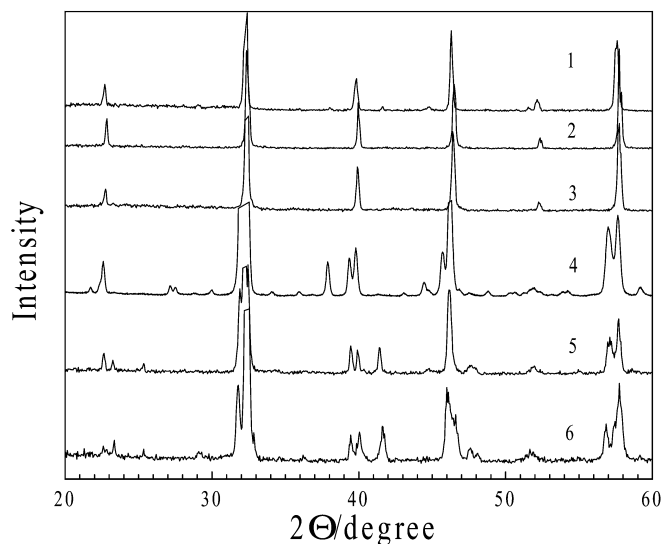


Fig. 2 X-ray powder diffraction patterns (Cu K α radiation) for the samples of $\text{La}_{1-x}\text{Sr}_x\text{FeO}_{3-\delta}$ fired at 700 °C in an atmosphere containing 5% H_2 and 95% He; $x=0.2$ (1), 0.4 (2), 0.5 (3), 0.7 (4), 0.9 (5) and 1.0 (6)

Table 2 Unit cell data at room temperature for specimens $\text{La}_{1-x}\text{Sr}_x\text{FeO}_{3-\delta}$ equilibrated at 700 °C and quenched in the gas mixture 5% H_2 /95% He

x	Symmetry	a (Å)	b (Å)	c (Å)
0.2	Orthorhombic	5.535(1)	5.558(1)	7.838(2)
0.4	Rhombohedral ^a	5.500(1)	–	13.588(3)
0.5	Rhombohedral	5.509(1)	–	13.596(1)
0.7	Orthorhombic	5.498(1)	11.862(3)	5.569(1)
0.9	Orthorhombic	5.625(1)	15.743(3)	5.526(1)
1.0	Orthorhombic	5.672(1)	15.576(3)	5.528(1)

^aHexagonal setting

General trends in conductivity

The logarithm of the total conductivity (σ) versus the logarithm of the oxygen partial pressure at different temperatures (T) are shown in Fig. 3 for the specimens $\text{La}_{1-x}\text{Sr}_x\text{FeO}_{3-\delta}$, where $x=0.2, 0.4, 0.5, 0.7$ and 0.9 . It should be noted that the overall time necessary for carrying out measurements for one specimen takes about 200–300 h. In contrast to other reports [2, 10], where the temperature interval above 900 °C was studied, the measurements in this study are in the range 750–950 °C. At the same time, our results and those of others [2, 10] are in good correspondence when the parameters T and $p\text{O}_2$ are the same and the doping levels are similar. The conductivity increase with pressure observed to the right of the minima of $\log \sigma$ vs. $\log p\text{O}_2$ shows that the majority charge carriers are electron holes. Thus σ_p dominates the total conductivity in the high-pressure limit. The respective conductivity changes with pressure are nearly proportional to $p\text{O}_2^{+1/4}$. The increase in conductivity with the pressure decrease, which is seen to the left of the minima, is indicative of electron-like charge

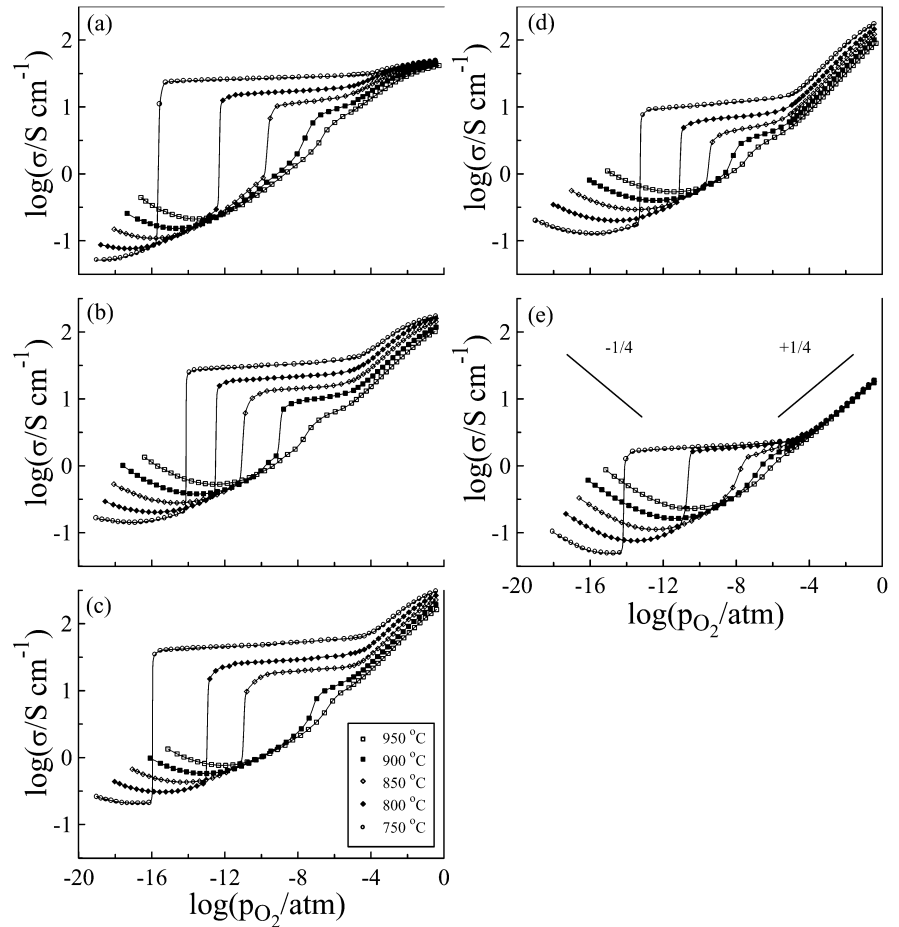
carrier contribution (σ_n) dominating the conductivity in the low-pressure extreme. The conductivity changes with pressure approach the $\sigma_n \approx p\text{O}_2^{-1/4}$ dependence.

Three distinctly different regions of the conductivity behavior can be observed. An example is given in Fig. 4, where the conductivity data at 850 °C are shown for $\text{La}_{0.5}\text{Sr}_{0.5}\text{FeO}_{3-\delta}$ as collected on decrease of the oxygen pressure (downward run) followed by an increasing upward run. Empty squares show results obtained under the equilibrium criterion as outlined in the Experimental section. A perfect match of the data in the downward and upward runs is seen in the high-pressure range (III), where according to Fig. 3 the conductivity is metal-like, and in the low-pressure range (I), where according to Fig. 3 the conductivity is temperature activated as in a semiconductor. Thus, in carrying out these experiments, the equilibrium criterion is quite sufficient to measure the equilibrium conductivity data in the pressure ranges I and III. The conductivity appears to depend on pressure only weakly in the intermediate pressure range (II), where there is a considerable difference in the values obtained in the downward and upward runs. Filled squares in Fig. 4 show the data taken after equilibration for 5 h at every pressure point. It is seen that the differences become just slightly smaller throughout the total measuring cycle at one temperature, which requires in excess of 200 h.

The relaxation data at 850 °C in Fig. 5 provide an additional illustration with respect to the origin of this peculiar behavior. It is seen clearly from Fig. 5a that the equilibration kinetics is so slow in the pressure range II that the conductivity values continue to change after 5 h of equilibration time with practically the same rate as at the start of the experiment. Therefore, the conductivity data points obtained in the range II, even at very lengthy isochronous measurements, do not quite correspond to equilibrium values. This is also the situation when measurements are carried out under the accepted equilibrium criterion in the conditions where the drift in the logarithm of the conductivity, which can be calculated from Fig. 5a, is in fact as slow as 0.01–0.02% per minute. Therefore, in order to obtain conductivity data in the range II, which are more close to equilibrium values, more stringent equilibration criteria, for example, a relative drift in the logarithm of the conductivity of about 0.001% per minute or even smaller, would be required. However, the measuring cycle of the conductivity at any one selected temperature would have taken an unreasonably long time of many hundreds of hours.

Quite in contrast, the equilibration time is relatively short in the pressure intervals I and III, as is evidenced by the example shown in Fig. 5b; equilibrium is attained after a reasonable equilibration times (0.5–3 h, after which the conductivity becomes practically independent of time, i.e. the conductivity change with time becomes smaller than the equilibrium criterion). Having achieved this state, the computer stores into memory the respective value that can be interpreted as the equilibrium conductivity at the given external parameters T and $p\text{O}_2$.

Fig. 3 Experimental results for changes in the total conductivity of $\text{La}_{1-x}\text{Sr}_x\text{FeO}_{3-\delta}$ with oxygen partial pressure at different temperatures; $x=0.2$ (a), 0.4 (b), 0.5 (c), 0.7 (d) and 0.9 (e). The temperature step between the isotherms is 50 °C



The very sluggish equilibration in the pressure range II may be related to the semiconductor-to-metal transition as proposed in published studies [18, 19]. However, there may be other processes, such as diffusion related to phase boundaries, surface reactions, etc. More complete understanding of the oxygen equilibration kinetics in the intermediate pressure range deserves a separate investigation. Here we utilize only the data obtained in the low-pressure range I for the analysis of the equilibrium conductivity in the ferrites.

The conductivity minima of the isotherms in Fig. 3 correspond to near equality of the electron (σ_n) and hole (σ_p) contributions. It is important to note that the conductivity changes with pressure near the minima are substantially smoother than expected from the sum of the electron and hole contributions only:

$$\sigma = \sigma_n^0 p\text{O}_2^{-1/4} + \sigma_p^0 p\text{O}_2^{+1/4} \quad (1)$$

This indicates the presence of one additional, pressure-independent, contribution to the conductivity. Such a contribution in the ferrites under consideration is due to the electric current formed by the movement of oxygen ions. Therefore, the experimental data around the minima were approximated with the expression:

$$\sigma(T, p\text{O}_2) = \sigma_i(T) + \sigma_n^0(T) p\text{O}_2^{-1/4} + \sigma_p^0(T) p\text{O}_2^{+1/4} \quad (2)$$

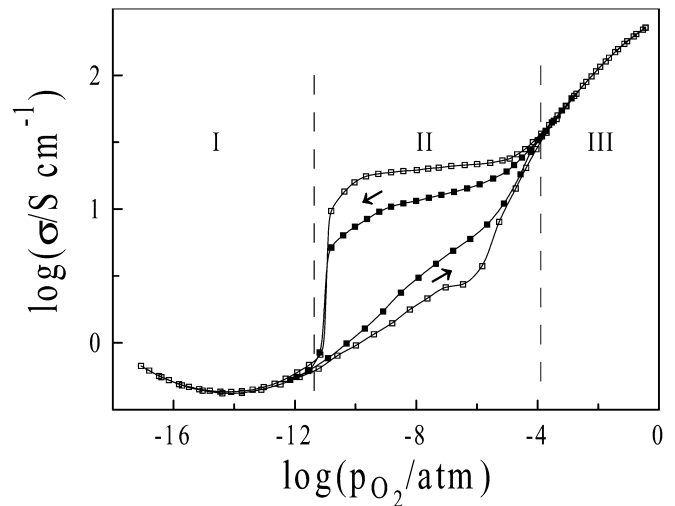


Fig. 4 The logarithmic plots of the conductivity versus oxygen partial pressure for $\text{La}_{0.5}\text{Sr}_{0.5}\text{FeO}_{3-\delta}$ at 850 °C. *Empty squares* show results measured under the accepted equilibrium condition, i.e. a conductivity drift smaller than 0.01% per minute. *Filled squares* show results taken at isochronous measurements during 5 h at any given value of pressure. *Arrows* show direction of the pressure changes during measurements

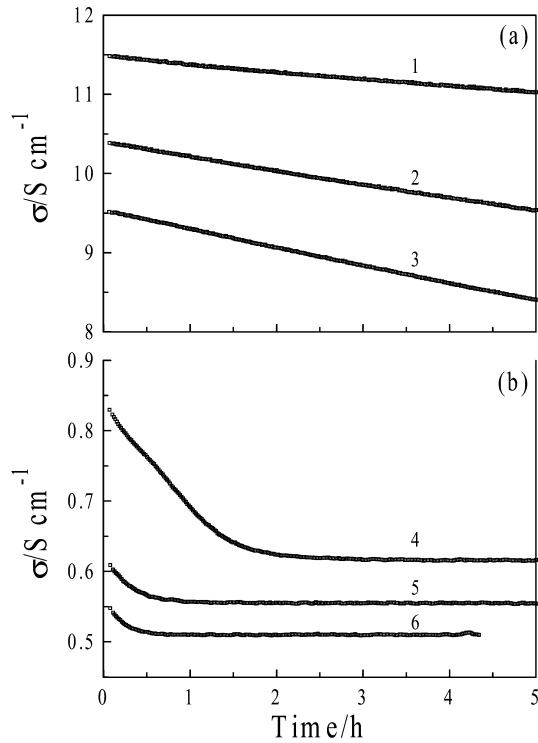


Fig. 5a, b The conductivity relaxation at the oxygen partial pressure decrease from 2.5×10^{-N} to 1×10^{-N} atm; $N=9$ (1), 10 (2), 11 (3), 12 (4), 13 (5) and 14 (6). Parts (a) and (b) show relaxation in regions II and I in Fig. 4, respectively. The time necessary to change pressure in the measuring cell did not exceed 20–30 s at any selected pressure

which is commonly applied for description of conductivity in oxygen ion-electron conductors [19]. Here, $\sigma_i(T)$ is the pressure-independent oxygen-ion contribution, while the coefficients $\sigma_n^o(T)$ and $\sigma_p^o(T)$ represent n- and p-type contributions, as extrapolated to $pO_2=1$ atm, respectively. Relation (2) enables one to quite precisely simulate the experimental data for different compositions and temperatures. The resulting ion conductivity values are summarized in Table 3.

Oxygen ion conductivity

The data in Table 3 may be utilized to plot the ion conductivity with Arrhenius coordinates (Fig. 6). It is seen that the ion conductivity attains a maximal value at $x=0.5$. Note also that the apparent activation energy for the ion conductivity (E_i) does not depend on strontium content at $x \leq 0.5$ (Table 4). Therefore, the acceptor content variations in this range do not effect the ion migration mechanism. This seems quite natural, because all compositions at $x \leq 0.5$ have the same perovskite-like structure. The ion conductivity dependence on strontium content $\sigma_i(x)$ is shown at 950 °C in Fig. 7. The increase of $\sigma_i(x)$ with x in the range $x \leq 0.5$ generally follows the oxygen vacancy increase. One may suppose, therefore, that the average oxidation state of iron is close

Table 3 Ion conductivity (S/cm) in $La_{1-x}Sr_xFeO_{3-\delta}$ at different temperatures

x	Temperature (°C)				
	950	900	850	800	750
0.2	1.01×10^{-1}	7.75×10^{-2}	5.93×10^{-2}	4.68×10^{-2}	3.41×10^{-2}
0.4	0.313	0.232	0.185	0.141	0.106
0.5	0.462	0.366	0.275	0.205	0.150
0.7	0.341	0.256	0.192	0.137	9.04×10^{-2}
0.9	1.24×10^{-1}	9.39×10^{-2}	6.14×10^{-2}	3.94×10^{-2}	2.34×10^{-2}

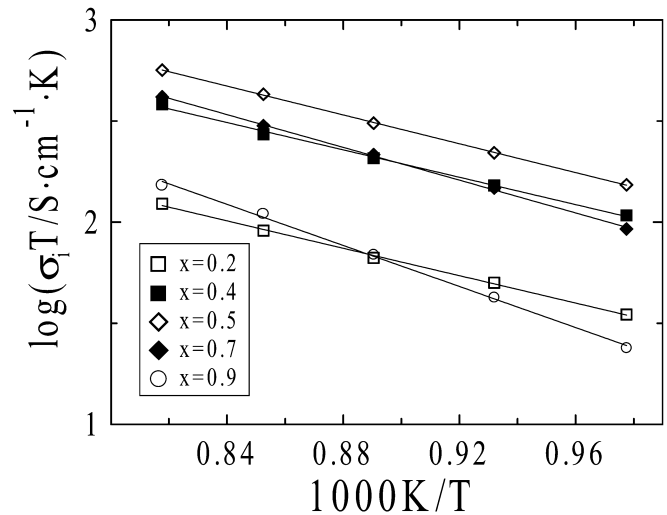


Fig. 6 Arrhenius plots for the ion conductivity in $La_{1-x}Sr_xFeO_{3-\delta}$

Table 4 Activation energy (eV) for the ion conductivity in $La_{1-x}Sr_xFeO_{3-\delta}$

x	0.2	0.4	0.5	0.7	0.9
E_i	0.67	0.67	0.7	0.8	1.0

to +3 in the experimental conditions used, or, in other words, the composition of ferrites with $x \leq 0.5$ remains close to the formula $La_{1-x}Sr_xFeO_{3-x/2}$ over the quite wide variations of oxygen activity in pressure range I. This reasonable supposition corresponds to primarily ionic compensation of acceptors, and it seems to be quite appropriate when the data are analyzed in the low oxygen pressures regime.

The dashed line in Fig. 7 depicts the concentration-dependent behavior of $\sigma_{\text{theor}} = \sigma^o(3-x/2)(x/2)$, where σ^o is a constant, as fitted by the least-squares method to experimental data at $x=0.2, 0.4$ and 0.5 . This theoretical dependence reflects changes in ion conductivity with acceptor concentration in a perovskite lattice having $(x/2)$ random vacancies and $(3-x/2)$ regular oxygen ions per elementary unit. The experimentally observed behavior generally follows this dependence at $x \leq 0.5$. Also, the line drawn over experimental points according to this dependence in the domain ($x \leq 0.5$) of the

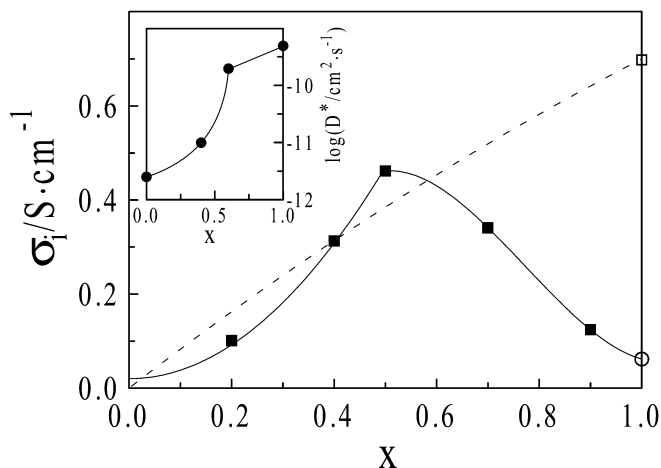


Fig. 7 Ion conductivity changes with strontium content in $\text{La}_{1-x}\text{Sr}_x\text{FeO}_{3-\delta}$ at 950 °C. The results shown with symbols (*open circles* and *open squares*) for the composition with $x=1$ are taken from [17] and [20], respectively. The *dashed line* shows approximation of the experimental data at $x=0.2, 0.4$ and 0.5 by the function $\sigma_i = \sigma^o(3-x/2)(x/2)$. The *inset* shows the data for the oxygen tracer diffusion coefficient from published work [9]

perovskite structure, and then extrapolated to $x=1$, gives the ion conductivity value in perfect match with the experimental result [21] obtained from permeation measurements at elevated temperatures and $p\text{O}_2 > 10^{-3}$ atm, i.e. in conditions where the ferrite $\text{SrFeO}_{3-\delta}$ has considerable oxygen deficiency ($\delta \rightarrow 0.5$) and simultaneously retains the structure of an oxygen vacancy disordered perovskite [22, 23].

The consistency of the ion conductivity values obtained by different methods in perovskite-like materials of $\text{La}_{1-x}\text{Sr}_x\text{FeO}_{3-\delta}$, in the low- and high-pressure limits, supports the reliability of our approach, which we have utilized in the determination of the ion contribution. Also, it demonstrates that the ion conductivity in the ferrites at a given temperature does not depend on oxygen pressure and is defined mainly by the oxygen vacancy concentration as long as the vacancies remain disordered.

It is shown above that oxygen vacancy ordering in oxides with $x > 0.5$ results in formation of layered structures characterized by alternation of iron-oxygen octahedra and tetrahedra in $\text{La}_{0.3}\text{Sr}_{0.7}\text{FeO}_{2.65}$ and $\text{La}_{0.1}\text{Sr}_{0.9}\text{FeO}_{2.55}$. It can be noticed that the ratio of octahedrally coordinated iron to tetrahedrally coordinated iron is larger in $\text{La}_{0.3}\text{Sr}_{0.7}\text{FeO}_{2.65}$ than in $\text{La}_{0.1}\text{Sr}_{0.9}\text{FeO}_{2.55}$. It is known also that oxygen ion transport in vacancy-ordered ferrites develops mainly in the layers of octahedra over vacancies (V_{oct}) formed as a result of anti-Frenkel disordering:



of oxygen anions in the layers of octahedra ($\text{O}_{\text{oct}}^{2-}$) and structural vacancies (V_{tet}) in the layers of tetrahedra [18, 19]. Hence, the general decrease of the ion conductivity in compositions with $x > 0.5$ compared to that in the oxide with $x=0.5$ and the greater decrease in the oxide

$x=0.9$ than in $x=0.7$ (see Fig. 7) appear to be a natural consequence of their local structures.

Additional data at 950 °C [18] are given in Fig. 7 for the brownmillerite-like ferrite $\text{SrFeO}_{2.5}$, where the relative amount of the ordered vacancies is larger than in $\text{La}_{0.1}\text{Sr}_{0.9}\text{FeO}_{2.55}$. Therefore, it is not surprising that the ion conductivity is somewhat smaller in $\text{SrFeO}_{2.5}$ than in $\text{La}_{0.1}\text{Sr}_{0.9}\text{FeO}_{2.55}$. As a whole, the concentration-dependent ion conductivity, $\sigma_i(x)$ in Fig. 7, demonstrates rather directly that an increase in the amount of random vacancies results in an increase of the ion conductivity. At the same time, an increase in the vacancy concentration favors a tendency for the vacancies to order, which in turn results in a lower number of available sites for oxygen transport. The tendency for the apparent activation energy to increase at $x > 0.5$, which can be seen in Table 4, shows again that the thermally activated ion transport in the vacancy-ordered phases $\text{La}_{0.3}\text{Sr}_{0.7}\text{FeO}_{2.65}$ or $\text{La}_{0.1}\text{Sr}_{0.9}\text{FeO}_{2.55}$ evolves on a background of a simultaneously developing disordering of structural vacancies [24].

Yet another feature in Fig. 7 attracts attention. Namely, the ion conductivity decrease with $x \rightarrow 0$ is somewhat faster compared to the dependence $\sigma_{\text{theor}} = \sigma^o(3-x/2)(x/2)$, which gives $\sigma_{\text{theor}} \approx x$ at small doping levels, while the experimentally observed behavior appears to follow more closely $\sigma_i \approx x^2$. In order to understand the reason for this deviation, it is important to recognize that along with the number of multipliers $(3-x/2)$ and $(x/2)$, which directly show the amount of migrating ions and number of vacancies available for ion jumps, respectively, there is a characteristic probability per unit time ω for the ion to jump that is related to the coefficient $\sigma^o \approx \omega$ [25]. This probability depends on the size of the “bottleneck” that must be overcome for the ion to jump from a regular site to the nearby vacancy. In ABO_3 perovskites this narrow space is framed by one B-type cation and two A-type cations and it would appear to be invariable at first glance. However, formation of oxygen vacancies in $\text{La}_{1-x}\text{Sr}_x\text{FeO}_{3-x/2}$ results in a decrease in the average coordination numbers for the La^{3+} , Sr^{2+} and Fe^{3+} cations and, therefore, to the proportional decrease of their average radii [26]. As a result, the average size of the “bottleneck” increases with vacancy concentration, i.e. with the doping level. Consequently, the jump probability must increase nearly proportionally to the doping level, that is $\omega \approx x$, and, therefore, changes in the ion conductivity follow a nearly parabolic dependence. These arguments are applied only to the case of random vacancies, which occur in the range $x \leq 0.5$.

Others [9] observed the same concentration-dependent behavior of the tracer diffusion coefficient D^* of oxygen in the ferrites with $x < 0.6$ (see inset in Fig. 7). Note that the tracer diffusion coefficient is related to the self-diffusion coefficient D as $D^* = f \times D$, where f is the correlation factor with a range of about unity in a perovskite-like lattice. Thus, this similarity ensues from the Nernst–Einstein relation that establishes the linear

relation of the kinetic coefficients D and σ . At larger strontium contents, the diffusion coefficient D^* tends to slightly increase with x while ion conductivity decreases. This apparent contradiction appears because the data reported previously [9] are obtained at high oxygen pressure ($pO_2 \approx 0.05$ atm) when strontium-rich ferrites adopt perovskite-like structures with random vacancies. The results in the present work are obtained at low oxygen pressure when the vacancy concentration achieves such large values that strontium-rich ferrites exhibit vacancy ordering and deterioration of the ion transport. Note additionally that our values $E_i \approx 0.7$ eV for the activation energy of the ion conductivity at $x \leq 0.5$ are very close to those for the diffusion activation energy at $x < 0.6$ [9]. At larger strontium content the conductivity activation energy $E_i \approx 0.8$ – 1.0 eV (Table 4) exceeds slightly the diffusion activation energy (~ 0.8 eV) reported [9]. This difference is related apparently to the vacancy ordering \leftrightarrow disordering effects that develop at low oxygen pressure, even at rather high temperatures, and strongly influence the ion conductivity in strontium-rich ferrites.

Conclusions

Electrical conductivity measurements of the ferrites $La_{1-x}Sr_xFeO_{3-\delta}$, where $x = 0.2, 0.4, 0.5, 0.7$ and 0.9 , were performed in the oxygen partial pressure range 10^{-19} – 0.5 atm and temperature varying between 750 and 950 °C. The oxygen ion conductivity values at different temperatures were obtained from the analysis of the pressure dependences of the total conductivity. The activation energy for the ion conductivity was determined at different acceptor contents. Complementary to the known literature for the high-pressure limit, the ion conductivity in the ferrites is shown to persist in the low-pressure extreme. It is argued that variations in the acceptor doping level and oxygen vacancy concentration result in structural modifications that develop simultaneously with changes in ionic conductivity.

Acknowledgements The work was carried out under contract 01-03-96519 with the Russian Foundation for Basic Research (RFBR). The authors appreciate partial support of this study by the NATO SfP Program under award 978002. One of us (K.R.P) is grateful to the EMSI program of the National Science Foundation and the U.S. Department of Energy Office of Science (CHE-9810378) at the Northwestern University Institute for Environmental Catalysis.

References

- Mizusaki J, Sasamo T, Cannon WR, Bowen HK (1982) *J Am Ceram Soc* 65:363
- Mizusaki J, Sasamo T, Cannon WR, Bowen HK (1983) *J Am Ceram Soc* 66:247
- Teraoka Y, Zhang H-M, Furukawa S, Yamazoe N (1985) *Chem Lett* 1743
- Mizusaki J, Ychihiro M, Yamauchi S, Fueki K (1985) *J Solid State Chem* 58:257
- Mizusaki J, Ychihiro M, Yamauchi S, Fueki K (1987) *J Solid State Chem* 67:1
- Dann SE, Currie DB, Weller MT, Thomas MF, Al-Rawwas AD (1994) *J Solid State Chem* 109:134
- Ishigaki T, Yamauchi S, Mizusaki J, Fueki K, Naito H, Adachi T (1984) *J Solid State Chem* 55:50
- Ishigaki T, Yamauchi S, Kishio K, Mizusaki J, Fueki K (1988) *J Solid State Chem* 73:179
- Kim MC, Park SJ, Haneda H, Tanaka J, Mitsuhashi T, Shirasaki S (1990) *J Mater Sci Lett* 9:102
- Kim MC, Park SJ, Haneda H, Tanaka J, Shirasaki S (1990) *Solid State Ionics* 40/41:239
- ten Elshof JE, Bouwmeester HJM, Verweij H (1995) *Solid State Ionics* 81:97
- ten Elshof JE, Bouwmeester HJM, Verweij H (1996) *Solid State Ionics* 89:81
- Patrakeev MV, Mitberg EB, Leonidov IA, Kozhevnikov VL (2001) *Solid State Ionics* 139:325
- Battle PD, Gibb TC, Lightfoot P (1990) *J Solid State Chem* 84:271
- Battle PD, Gibb TC, Lightfoot P (1990) *J Solid State Chem* 84:277
- Grenier JC, Ea N, Pouchard M, Hagenmuller P (1985) *J Solid State Chem* 58:243
- Schmidt M, Campbell SJ (2001) *J Solid State Chem* 156:292
- Kozhevnikov VL, Leonidov IA, Patrakeev MV, Mitberg EB, Poeppelmeier KR (2001) *J Solid State Chem* 158:320
- Leonidov IA, Kozhevnikov VL, Patrakeev MV, Mitberg EB, Poeppelmeier KR (2001) *Solid State Ionics* 144:361
- Bouwmeester HJM, Burggraaf AJ (1996) In: Burggraaf AJ, Cot L (eds) *Fundamentals of inorganic membrane science and technology*. Elsevier, Amsterdam, pp 435–528
- Teraoka Y, Zhang HM, Furukawa S, Yamazoe N (1988) *Chem Lett* 7:1084
- Takeda Y, Kanno K, Takada T, Yamamoto O, Takano M, Nakayama N, Bando Y (1986) *J Solid State Chem* 63:237
- Mizusaki J, Okayasu M, Yamauchi S, Fueki K (1992) *J Solid State Chem* 99:166
- Shilova YA, Patrakeev MV, Mitberg EB, Leonidov IA, Kozhevnikov VL, Poeppelmeier KR (2002) *J Solid State Chem* 168:275
- Shewmon PG (1967) *Diffusion in solids*. Williams, LOCA-TION????
- Shannon RP (1976) *Acta Crystallogr Sect A* 32:751